JHK_s time-series observations of a few ultracool dwarfs

C. Koen,[1,2]★ T. Tanabé,[3] M. Tamura[4] and N. Kusakabe[5]

[1]*Department of Statistics, University of the Western Cape, Private Bag X17, Bellville 7535, Cape, South Africa*
[2]*South African Astronomical Observatory, PO Box 9, Observatory 7935, Cape, South Africa*
[3]*Institute of Astronomy, School of Science, The University of Tokyo, Mitaka, Tokyo 181-0015, Japan*
[4]*National Astronomical Observatory of Japan, Mitaka, Tokyo 181-8588, Japan*
[5]*Tokyo Gakugei University, Koganei, Tokyo 184-8501, Japan*

ABSTRACT

The M8.5 object SSSPM J0109−5101 has recently been shown to be both a periodic and a flaring variable, based on optical observations in the extreme red. More than 16 h of monitoring in the near-infrared (NIR) reported here failed to show any variability. Similarly, no NIR variability could be detected in intensive monitoring of three other suspected optical variables. This paper also reports on photometry of half a dozen targets monitored over a few weeks, and on the comparison of intensive monitoring at different epochs. In only one case, that of the T dwarf binary ϵ Indi Bab, is there good evidence for variability. Our results allow stringent limits to be placed on the NIR variability levels in a large sample of ultracool dwarfs.

Key words: techniques: photometric – stars: individual: ϵ Indi Bab – stars: individual: SSSPM J0109−5101 – stars: low-mass, brown dwarfs – stars: variables: other.

1 INTRODUCTION

Koen et al. (2004, Paper I) monitored 18 objects with spectral classifications of L or T for a few hours each in JHK_s, and found no variability in excess of about 0.02 mag. This result contrasts with earlier studies of other objects (see Paper I for references) in which substantial near-infrared (NIR) variability was reported, although usually on somewhat longer time-scales. In an attempt to shed more light on the question of NIR variability, the present paper contains the results of three rather disparate studies. First, it is possible that objects that are known to be variable in the optical will vary on similar time-scales in the NIR. Four targets with fairly short confirmed or suspected optical periods were therefore chosen for more intensive NIR monitoring. Secondly, we obtained a few observations, spread over an interval of about three weeks, on each of half a dozen targets: this was intended to provide information about variability on time-scales of days. Thirdly, for a few objects the results of a few hours of monitoring at different epochs are available. This is valuable, as mean brightnesses at the different epochs can be calculated to very good accuracy and compared.

The observations of the known variable, SSSPM J0109−5101, and the three suspected variables, 2M 2130−0845, 2M 2104−0845 and DENIS 0255−4700, are plotted and analysed in Section 4 of the paper. This material forms the bulk of the new photometry reported on here. Relevant information (infrared magnitudes and spectral classifications) and the observing log are given in Table 1. The details

were obtained from the DwarfArchives.[1] We note one change: the original L2 spectral classification of SSSPM J0109−5101 (Lodieu, Scholz & McCaughrean 2002) has been revised to M8.5 (Lodieu, private communication).

Table 2 contains similar information for the nightly targets; the observations are dealt with in Section 5. The multi-epoch data are discussed in Section 6 (objects listed in Table 3).

Data acquisition and reduction are described in the next section of the paper. Section 3 is concerned with the combination of data from different nights, i.e. the calculation of zero-point differences, for which we use a somewhat unconventional approach. Conclusions are presented in Section 7.

The IAU recommended names of the objects studied in this paper are rather long, and we chose to abbreviate most below, as follows:

2M 0030−1450	= 2MASSI J0030300−145033,
	= 2MASSW J0030300−145033
DENIS 0255−4700	= DENIS-P J025503.5−470050
SDSS 0330−0025	= SDSS J033035.13−002534.5
SDSS 0423−0414	= SDSS J042348.57−041403.5
2M 1225−2739AB	= 2MASS J12255432−2739466[AB]
2M 1534−2952AB	= 2MASS J15344984−2952274[AB]
2M 2104−1037	= 2MASS J21041491−1037369
2M 2130−0845	= 2MASS J21304464−0845205
2M 2224−0158	= 2MASS J22244381−0158521

★E-mail: ckoen@uwc.ac.za

[1] http://spider.ipac.caltech.edu/staff/davy/ARCHIVE

2 OBSERVATIONS AND REDUCTIONS

All observations were made with the SIRIUS camera attached to the 1.4-m Infrared Survey Facility (IRSF) telescope, situated at Sutherland, South Africa. The observing setup and basic reduction techniques used were virtually identical to those in Paper I, to which the interested reader is referred for details: here we mention only three minor differences. First, the field of view of the camera has been more accurately determined as 7.7×7.7 arcmin^2. Secondly, the dithering pattern consisted of 10 positions, rather than nine. Thirdly, flat-field exposures were obtained during each clear evening and morning twilight, and all exposures for the preceding week of observing were combined to maximize the accuracy.

3 COMPARING RESULTS FROM DIFFERENT NIGHTS

In order to compare measurements from different nights, it is necessary to determine zero-point differences. Formally, the following procedure could be used: Let v_{jk} be the mean magnitude of star k during night j. Refer the zero-point offsets Z_j for all other nights to night 1:

$$v_{jk} = v_{1k} + Z_j + e_{jk},$$

where e_{jk} is the 'error', with estimated variance S_{jk}^2. The weighted least-squares estimator for Z_j is then

$$z_j = \frac{\sum_{k=1}^{K}(v_{jk} - v_{1k})S_{jk}^{-2}}{\sum_{k=1}^{K} S_{jk}^{-2}}, \tag{1}$$

which has standard error

$$\text{s.e.}(z_j) \approx \left(\sum_{j=1}^{K} S_{jk}^{-2} \right)^{-1/2}. \tag{2}$$

In (1) and (2), K is the number of stars common to the two nights.

If the magnitude of star k was measured N_{jk} times during night j, with estimated scatter s_{jk} around its mean value, then a natural estimator for the variance of e_{jk} is

$$S_{jk}^2 = \frac{s_{jk}^2}{N_{jk}} + \frac{s_{1k}^2}{N_{1k}}. \tag{3}$$

In practice, it may be expected that some of the stars will not be suitable for use as zero-point determinants. In particular, variables may show large changes in mean magnitude between different nights. A mechanism for weeding out such stars is required. If all is well with the theory above, then it may be expected that for reasonably large N_{jk} the quantities

$$\Delta_{jk} = \frac{v_{jk} - v_{1k} - Z_j}{S_{jk}} \qquad \text{for } k = 1, 2, \ldots, K \tag{4}$$

would have a distribution close to the standard normal (i.e. a Gaussian with zero mean and unit variance) for constant stars. Large-amplitude variables, on the other hand, could have large values of $|\Delta_{jk}|$ associated with them. A cut-off, say in the range 3–4, could then be used to eliminate unsuitable stars.

Unfortunately, experience has shown that the distribution of Δ_{jk} can be very far from a standard Gaussian, with an excess of large absolute values. Investigation of the reasons is outside the scope of this paper, although we speculate that S_{jk}^2 as calculated from (3) severely underestimates the error variance. Of course, (3) takes no direct account of systematic errors; it reflects primarily random errors.

A further consequence of the distinct non-normality of the Δ_{jk} is that standard tests for a change in the mean brightness cannot be applied.

We introduce the following simple ad hoc alternative to the procedure above: First, as a preliminary, the nightly zero-points are adjusted so that the ultracool object has the same mean magnitude for all nights. The differences

$$d_{jk} = v_{jk} - v_{1k}$$

in the mean magnitudes are then calculated for all other stars, and objects for which $|d_{jk}| > 0.1$ mag are rejected as unsuitable for zero-point determination. Further rejections can be based on iteratively removing stars with outlying absolute values of

$$\Delta_{jk}^* = \frac{d_{jk} - \overline{d}_j}{S_j^*}, \tag{5}$$

where

$$\overline{d}_j = \frac{1}{K} \sum_{k=1}^{K} d_{jk} \qquad \text{and} \qquad S_j^* = \sqrt{\frac{1}{K} \sum_{k=1}^{K}(d_{jk} - \overline{d}_j)^2}.$$

The zero-point offset for night j is then simply calculated as $z_j = \overline{d}_j$, where the mean is taken over all remaining stars.

A little reflection shows that the estimated mean magnitude difference for the target object is $-z_j$, since the mean values for the ultracool dwarf were set equal for the two nights. A rough idea of the significance of this estimated change can then be gained by noting the percentile position of $|z_j|/S_j^*$ with respect to the Δ_{jk}^* for stars with $|d_{jk}| < 0.1$.

Table 4 contains the results of applying this methodology to the data sets listed in Tables 1 and 3.

4 RESULTS OF INTENSIVE MONITORING

The bulk of the data analysed in this paper are displayed in Figs 1–3 (SSSPM J0109−5101), Figs 4 and 5 (2M 2130−0845), Fig. 6 (2M 2104−1037) and Fig. 7 (DENIS 0255−4700). (In all these and similar diagrams, differential magnitudes are plotted with respect to their nightly mean values.) Inspection of these diagrams shows very little sign of variability, except possibly in the K_s band. However, a glance at the comparison star data for the latter filter generally reveals trends of similar extent to those of the ultracool dwarf data, which leaves no convincing evidence for brightness changes. We proceed to quantitative analysis to test for the presence of low-level periodicities.

4.1 SSSPM J0109−5101

Strong optical (R and I band) flares in the M8.5 star/brown dwarf SSSPM J0109−5101 were discovered by Koen (2005a). The object also showed sinusoidal variations with a period of 7.8 h (frequency 3.07 d^{-1}) and semi-amplitude of 19 mmag in the I band.

Neither the zero-point shifts between HJD 245 3277 and 245 3278 nor between HJD 245 3277 and 245 3280 appeared to be meaningful. The small estimated shifts were in the same directions in the two cases (for all three filters), which implies that the differences between HJD 245 3277 and 245 3280 were even less significant. None
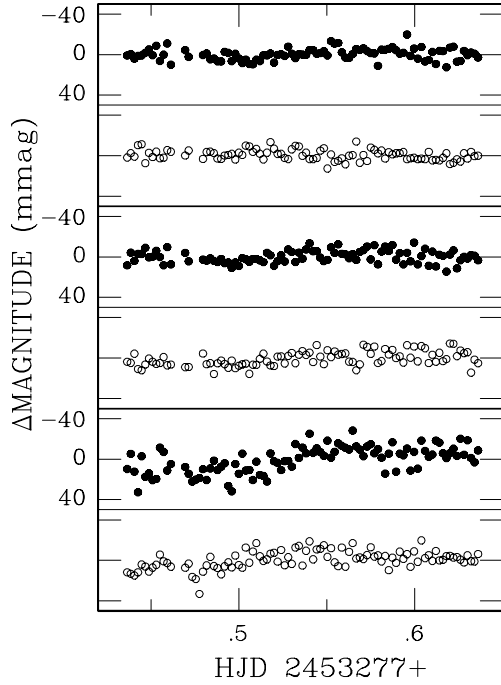
Figure 1. Results for the first run on SSSPM J0109−5101. The top two panels show the *J*-band observations of SSSPM J0109−5101 (filled symbols) and a local standard of similar brightness (open symbols). Similarly, the two middle panels show the results for *H*, and the bottom panels for *K*ₛ.
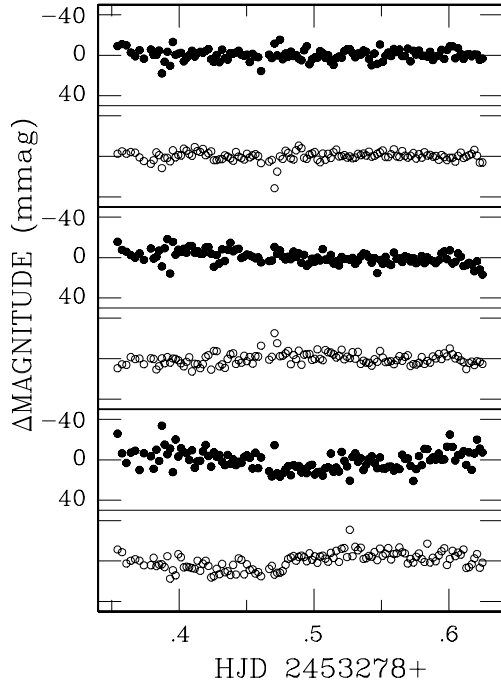
Figure 3. Results for the third run on SSSPM J0109−5101. See Fig. 1 caption for an explanation of what is plotted in the various panels.

Figure 2. Results for the second run on SSSPM J0109−5101. See Fig. 1 caption for an explanation of what is plotted in the various panels.

Figure 4. Results for the first run on 2M 2130−0845. See Fig. 1 caption for an explanation of what is plotted in the various panels.

the less, we prefer to err on the side of caution (particularly as *z* had the same sign for all filters), and apply the estimated zero-point shifts before applying period-finding techniques.

A look at the last column of Table 1 shows that the scatter in the light curves of SSSPM J0109−5101 is quite small, particularly in the *J* and *H* bands. Of course, the systematic nature of periodic
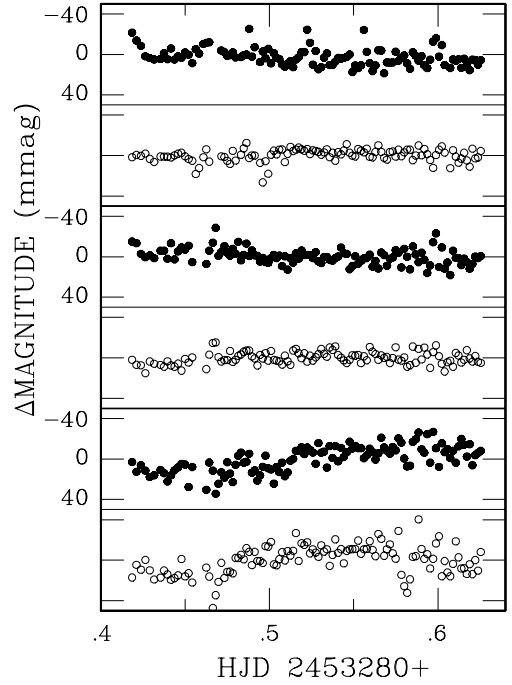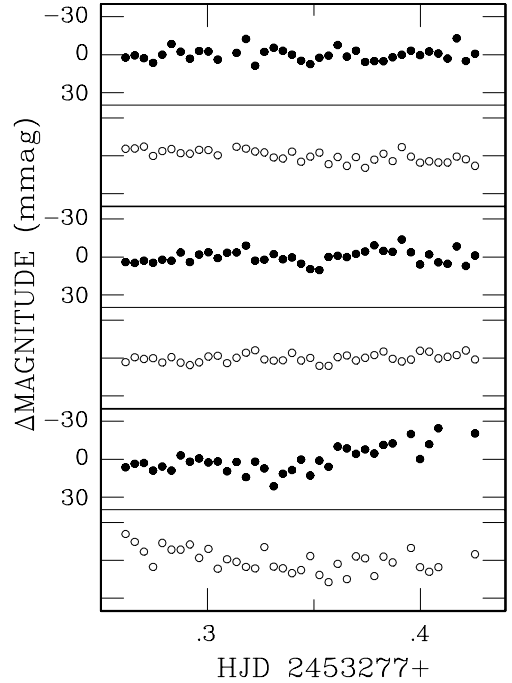
brightness changes allows one to detect variability at even lower levels. Two different period-finding methods were tried on the data in Figs 1–3: first, Fig. 8 shows the Fourier amplitude spectrum for each of the three data sets, after applying the zero-point corrections given in Table 4. The only reasonably close correspondence between the spectra for the three different filters is near 2.6 d⁻¹, but it is far from convincing. The distinguishing feature of the second method
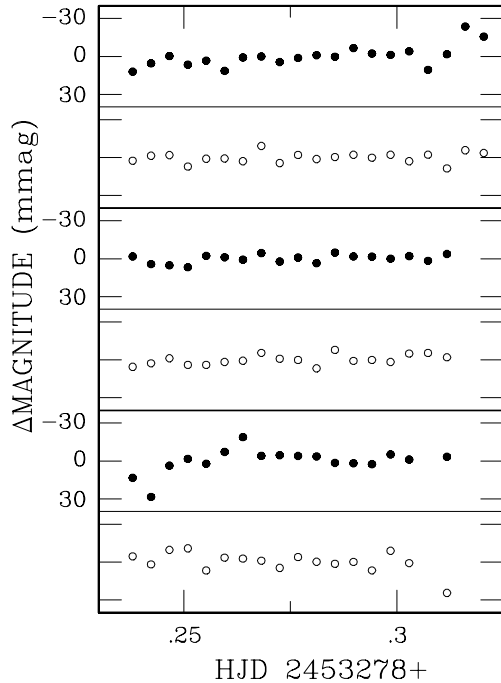
Figure 5. Results for the second run on 2M 2130−0845. See Fig. 1 caption for an explanation of what is plotted in the various panels.
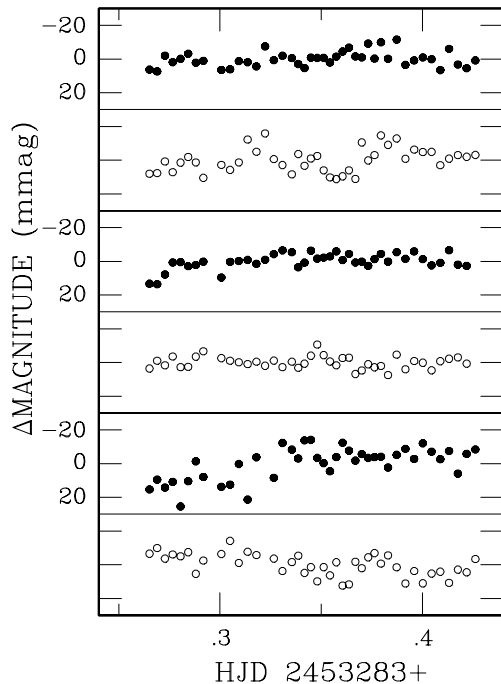

Figure 6. Results for the run on 2M 2104−1037. See Fig. 1 caption for an explanation of what is plotted in the various panels.

is that it allows for possible shifts in the mean light level of the dwarf which are intrinsic to the object: an amplitude, phase and frequency, as well as nightly mean levels, are all fitted simultaneously to the data by least squares (Koen 2003, 2004). The sum of squared residuals (RSS) is plotted in Fig. 9 for the same frequency range as for the amplitude spectra. The only noteworthy feature close to
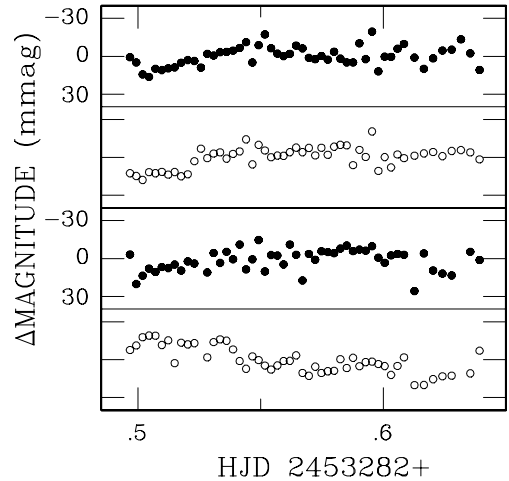

Figure 7. Results for the run on DENIS 0255−4700. The top two panels show the *H*-band observations of DENIS 0255−4700 (filled symbols) and a local standard of similar brightness (open symbols). Similarly, the two middle panels show the results for K_s.

the 3 d^{-1} frequency present in the optical data is in the K_s-band panel.

We conclude that there is no sign in the NIR of the periodicity detected in the *I* band less than two weeks prior.

4.2 2M 2130−0845

There is evidence in optical photometry (Koen 2005b) for short (<2 h) period variability in 2M 2130−0845. On the other hand, a null result was reported in Paper I, based on 3.7 h of JHK_s monitoring.

The two types of frequency spectra, calculated for the data in Figs 4 and 5, are plotted in Figs 10 and 11. The *H*-band data do show substantial power in the range 10–17 d^{-1}, but there are no corresponding features in the data for the two other filters. Residual sum of squares spectra for the earlier JHK_s data are plotted in fig. 22 of Paper I: those also show disagreement between the results for different filters.

The data from the two nights were also studied separately: the most telling result was the fact that substantial power in the range quoted above is present in the *H*-band data during only the first night. Conclusions similar to those for SSSPM J0109−5101 therefore apply.

4.3 2M 2104−1037

Marginal evidence for a ∼1.6-h periodicity in *H* and K_s data was presented in Paper I. The residual sum of squares spectra of the present data are plotted in Fig. 12; the upper curve is the inverse variance weighted sum (SRSS) of the three curves in the bottom panel (see Paper I for details). There is no sign of the periodicity tentatively identified in Paper I.

4.4 DENIS 0255−4700

There is evidence for variability in optical photometry of this object (Koen 2005b). The residual sum of squares spectra for the *H* and K_s data, and their weighted combination, are plotted in Fig. 13 (the *J*-band data were not usable). Clearly there is no periodicity common to the two filters. The best frequency of 6.7 d^{-1} derived from the

Table 1. Pertinent target data and observing log. Infrared photometry and spectroscopic classifications were taken from the website mentioned in the footnote in the Introduction. Columns 8 and 9 show the integration time T_{int} in each individual exposure, and the maximum number of combined exposures (each consisting of 10 dithers) obtained in any filter. The last column is the standard deviation of all measurements in each of the filters.

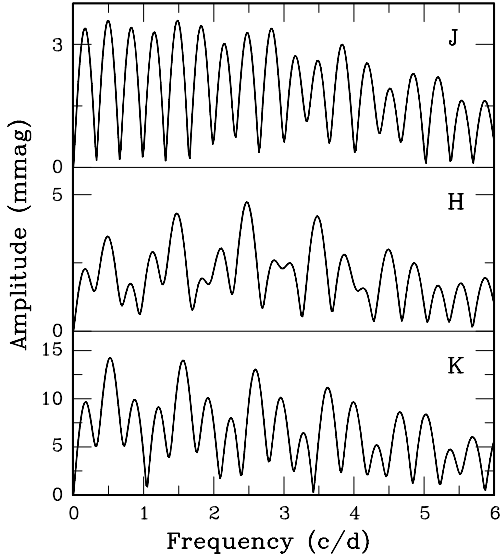| Name	J	H	K_s	Sp.	Start (HJD 245 3270+)	Run length (h)	T_{int} (s)	N(max)	$\sigma(J), \sigma(H), \sigma(K_s)$ (mmag)
SSSPM J0109−5101	12.23	11.54	11.09	M8.5	7.44	4.8	10	96	6, 6, 13
					8.35	6.5	20	127	5, 6, 10
					10.42	5.0	7–15	114	9, 8, 13
DENIS 0255−4700	13.23	12.19	11.53	L8	12.50	3.4	15–25	52	∗, 8, 9
2M 2104−1037	13.84	12.98	12.37	L2.5	13.27	3.9	20–30	42	6, 5, 10
2M 2130−0845	14.14	13.33	12.82	L1	7.26	3.9	30	39	5, 5, 10
					8.24	2.0	30	20	8, 3, 9

Figure 8. Amplitude spectra of the SSSPM J0109−5101 data in Figs 1–3, over the frequency range containing dominant peaks.
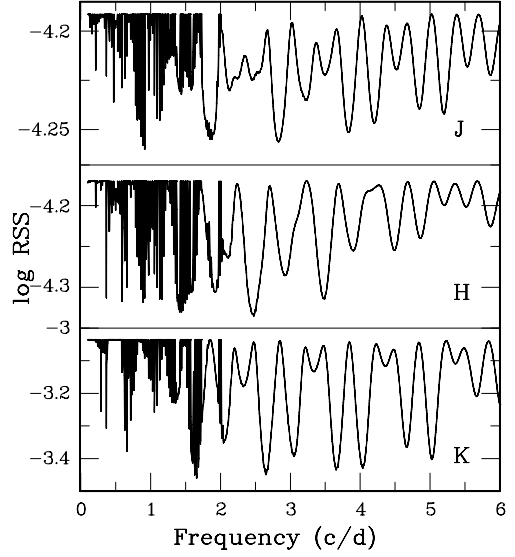

Figure 9. RSS spectra (see text) of the SSSPM J0109−5101 data in Figs 1–3, over the frequency range containing dominant features.

combined spectra corresponds to a period comparable to the run length.

5 RESULTS OF NIGHTLY OBSERVATIONS

The six targets listed in Table 2 were observed 1–3 times per night over intervals of about three weeks. The number of nights on which a particular object was observed ranged from four to eight. The results are shown in Figs 14–19. As measured against the comparison star data, none of the ultracool dwarfs show evidence for either substantial night-to-night scatter, or for systematic longer-term variability.

Two of the ultracool dwarfs listed in Table 2 have been previously observed in the NIR. Enoch, Brown & Burgasser (2003) found a possible sinusoidal variation (period ∼1.5 h, semi-amplitude ∼0.1 mag) in about 30 K_s-band observations of 2M 0030−1450 spread over 10 nights. Monitoring of 2M 0423−0414 of similar extent led to a conclusion that it was a 'possible detection' as a variable. Enoch et al. (2003) quote 'detection limits' of 0.20 and 0.11 mag for random variability in 2M 0030−1450 and 0423−0414, respectively. Our data do not confirm brightness changes in either of these objects. We note also that Artigau, Nadeau & Doyon (2003) did not find significant variability in their J-band photometry of 2M 0423−0414.
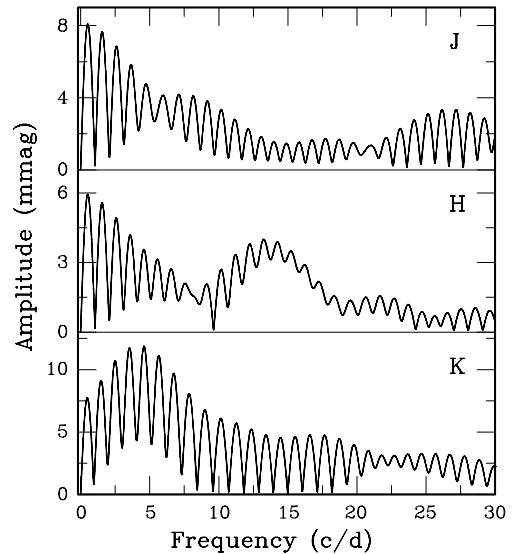

Figure 10. Amplitude spectra of the 2M 2130−0845 data in Figs 4 and 5, over the frequency range containing dominant peaks.
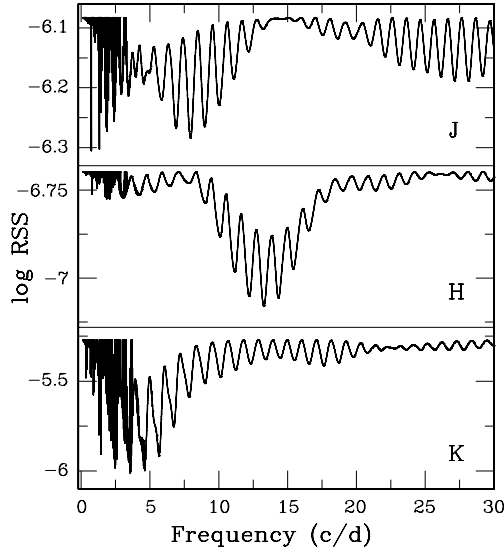
Figure 11. RSS spectra (see text) of the 2M 2130−0845 data in Figs 4 and 5, over the frequency range containing dominant features.
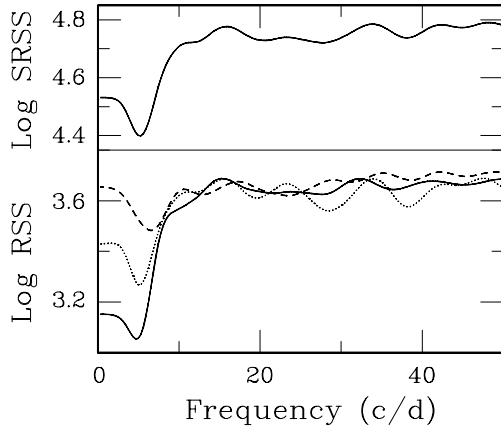

Figure 12. The results of fitting sinusoids with frequencies in the range 0–50 d^{-1} to the measurements of 2M 2104−1037. The bottom panel shows the scaled residual sum of squares for K_s (solid line), H (dotted line) and J (dashed line). The top panel shows the sum of the three curves in the bottom panel.

6 COMPARISON OF MEAN MAGNITUDES AT DIFFERENT EPOCHS

Some of our targets have been measured repeatedly at more than one epoch. In principle, this allows us to detect very small changes in mean brightness on longer time-scales. The data at our disposal are summarized in Table 3: these include material from Paper I, the present paper, and lower-quality unpublished photometry. The results of applying the method in Section 2 to these data are given in Table 4.

Only six of the crude significance levels in Table 4 are better than 10 per cent, one for 2M 2104−1037, two for 2M 2130−0845, and three for ϵ Indi Bab. In the case of 2M 2104−1037, the J-band zero-point is fainter at a marginally significant level in the latest observations, implying that the dwarf may have brightened (by about 23 mmag). It is noteworthy that the estimated zero-points for H and K_s are also both fainter. In the case of
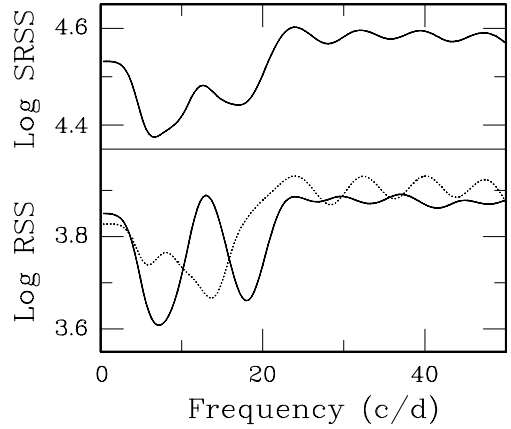

Figure 13. The results of fitting sinusoids with frequencies in the range 0–50 d^{-1} to the measurements of DENIS 0255−4700. The bottom panel shows the scaled residual sum of squares for H (dotted line) and K_s (solid line). The top panel shows the sum of the H and K_s curves.
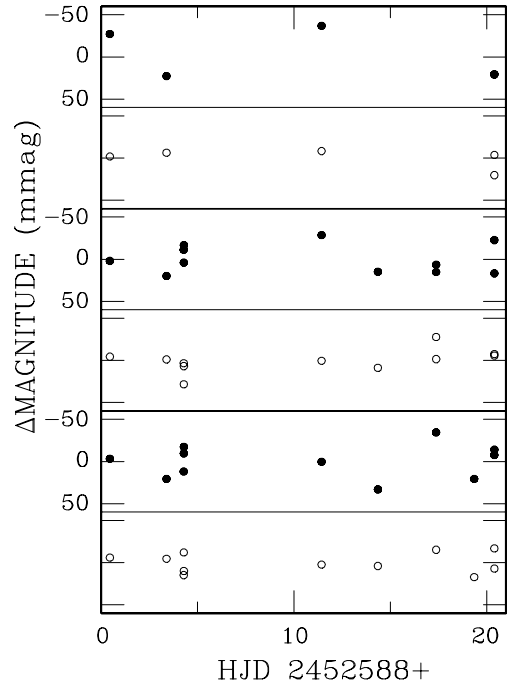

Figure 14. Nightly photometry of 2M 0030−1450. The top two panels show the results for the programme object (filled symbols) and a comparison star of similar brightness (open symbols). Similarly, the two middle panels show the results for H, and the bottom panels for K_s.

2M 2130−0845, both J and H magnitudes are brighter on HJD 245 3278 than on HJD 245 2805; the K_s magnitude is also brighter, though at a lower level. We consider these results, particularly those for 2M 2130−0845, to be encouraging, though hardly conclusive.

As far as ϵ Indi Bab is concerned, it was significantly ($\alpha =$ 4 per cent) fainter in the K_s band by an estimated 57 mmag on HJD 245 3281, as compared to HJD 245 2803. This is confirmed by a comparison of the K_s-band brightnesses on HJD 245 2803 and 245 3282: the estimated dimming is 53 mmag ($\alpha = 3$ per cent).

Table 2. Pertinent target data and observing log for nightly observations. See Table 1 caption for a description of the first five, and the last, columns of the table. The figure given under 'Nights' is the number of nights during which measurements were obtained.

| Name	J	H	K_s	Sp.	Interval covered (HJD 245 0000+)	Nights	N(max)	$\sigma(J), \sigma(H), \sigma(K_s)$ (mmag)
2M 0030−1450	16.79	15.36	14.38	L7	2588–2608	8	11	26, 16, 19
SDSS 0330−0025	15.29	14.42	13.83	L2:	2588–2608	8	10	14, 18, 21
SDSS 0423−0414	14.45	13.44	12.94	T0	2588–2608	8	10	15, 11, 2
2M 1225−2739AB	15.26	15.10	15.07	T6	2764–2775	4	7	12, 14, 9
GJ 570 D	15.33	15.28	15.27	T8	2764–2780	6	10	26, 19, 23
2M 1534−2952AB	14.90	14.89	14.86	T5.5/T5.5	2764–2780	5	11	10, 11, 18
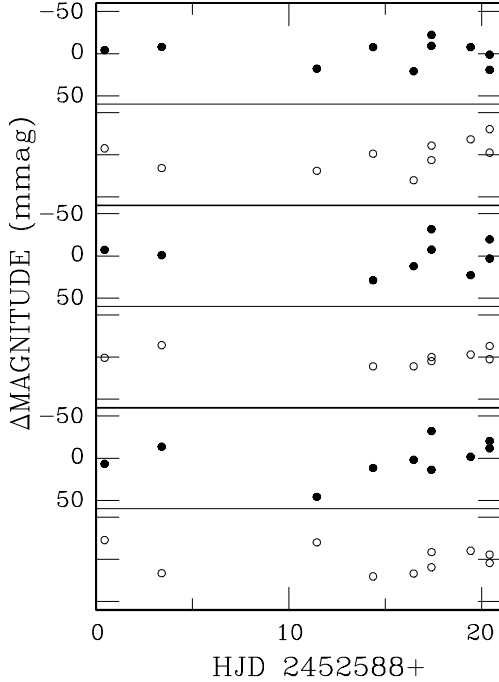
Figure 15. Nightly photometry of SDSS 0330−0025. See Fig. 14 caption for an explanation of what is plotted in the various panels of the diagram.
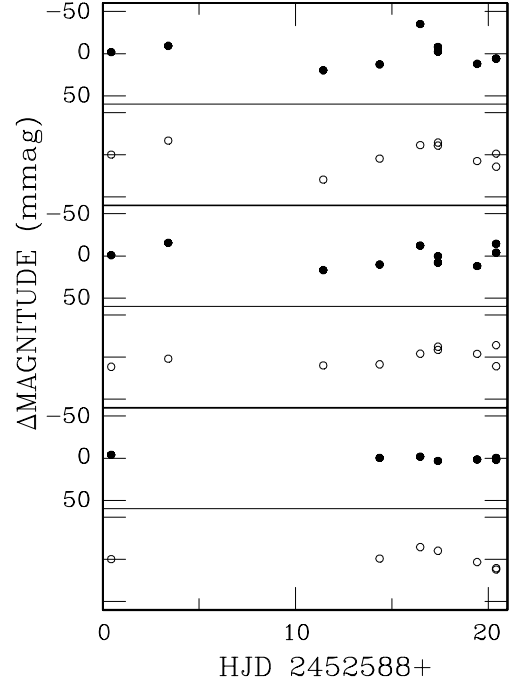

Figure 16. Nightly photometry of SDSS 0423−0414. See Fig. 14 caption for an explanation of what is plotted in the various panels of the diagram.

Furthermore, *H*-band magnitudes are available for both of the latter two nights, and the dimming of 34 mmag is significant at the 7 per cent level. The K_s-band data are plotted in Fig. 20.

Gelino et al. (2002) obtained 15 *I*-band measurements of 2M 2224−0158, spread over five nights. The mean error level of the photometry was 0.057 mag, and the standard deviation of the ultracool dwarf light curve 0.083 mag. The programme object was classified as 'variable' on the basis of a χ^2 test. We cannot confirm variability in this object.

7 DISCUSSION AND CONCLUSIONS

A major conclusion of Paper I was that none of the 18 ultracool objects each monitored for 2–4 h showed variability exceeding the 0.02 mag level. The JHK_s differential photometry presented here should be seen as an extension of that result: the only object for which we find reasonably convincing evidence of NIR variability is ϵ Indi Bab, which appeared substantially (∼0.05–0.06 mag) fainter

in 2004 October (HJD 245 3281) than in 2003 June (HJD 245 2803). In particular, the observations described in Section 4 are essentially null results, despite the fact that the targets have been shown to be variable in the optical on short time-scales.

In the case of SSSPM J0109−5101, the present result is based on more than 300 measurements obtained during 16 h of photometry. Despite the fact that frequent, and large, flares were observed in the optical (Koen 2005a), none were seen in the present study. This may be understandable given that flare amplitudes in M dwarfs are observed to decrease with increasing wavelength (e.g. Butler 1991). Perhaps more noteworthy is that there is no sign in the NIR of the sinusoidal variations seen in the *R* and *I* bands (cf. Figs 1–3, 8 and 9).

The strongest evidence for NIR variability that we have found to date is the differences of ∼0.03 mag in *H* and ∼0.05 mag in *K* in observations of ϵ Indi Bab at different epochs. It is tempting to deduce that this system may vary on long time-scales. This is not necessarily the case. Although rapid variability has not been seen in the NIR, it has certainly been observed in the optical. For example,
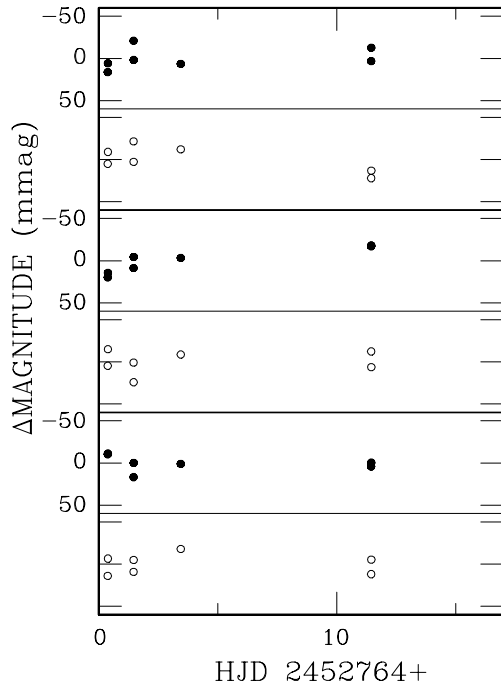
Figure 17. Nightly photometry of 2M 1225−2739AB. See Fig. 14 caption for an explanation of what is plotted in the various panels of the diagram.

Figure 18. Nightly photometry of GJ 570D. See Fig. 14 caption for an explanation of what is plotted in the various panels of the diagram.

Koen (2005b) found a brightening of more than 0.1 mag in 3.6 h of *I*-band monitoring. On the other hand, other runs in the optical saw far less activity (Koen 2003). Monitoring at different time-scales is required to resolve the nature of its variability.
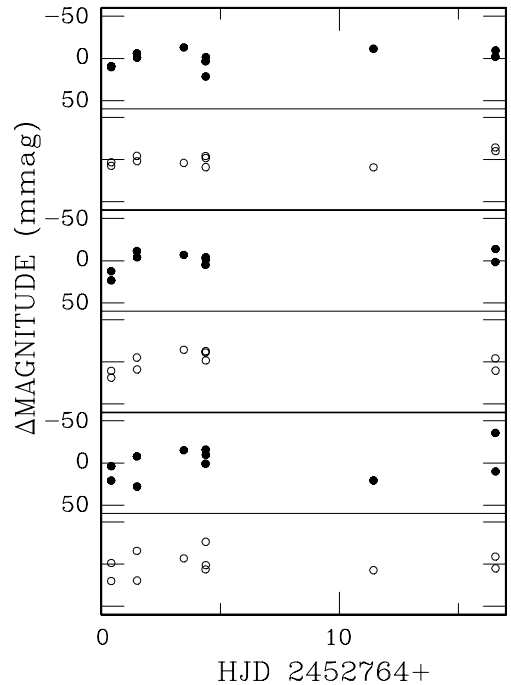

Figure 19. Nightly photometry of 2M 1534−2952AB. See Fig. 14 caption for an explanation of what is plotted in the various panels of the diagram.
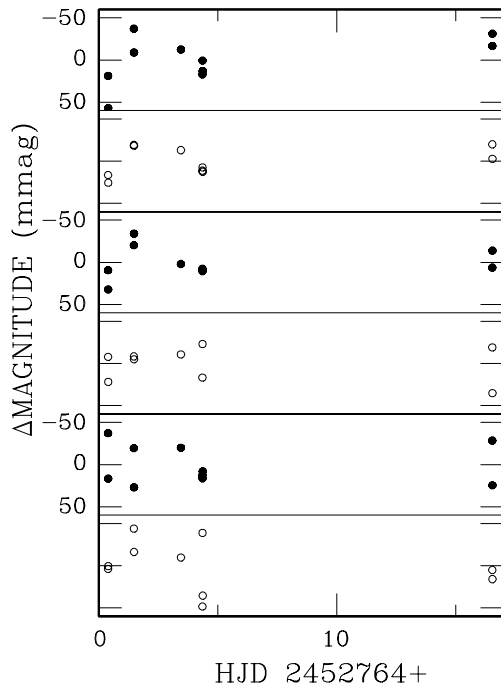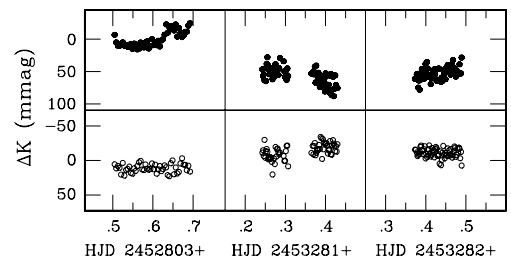

Figure 20. The K_s photometry of ϵ Indi Bab obtained at three epochs (top panels). The bottom panels show the corresponding measurements of a comparison star in the field of view.

We conclude with a cautionary note. It has been implicitly assumed above that any variability in the *J*, *H* and K_s bands would be similar. However, this may not be the case. A favoured explanation of photometric variability in field ultracool dwarfs is the effects of the evolution of dust cloud patterns in their atmospheres (e.g. Bailer-Jones & Mundt 2001; Gelino et al. 2002). The theory of such weather patterns in low-mass astronomical objects is discussed by Schubert & Zhang (2000); see also Burgasser et al. (2002). Given the complexity of the vertical distribution of particles in the atmosphere (e.g. Ackerman & Marley 2001; Burgasser et al. 2002; Woitke & Helling 2004; Tsuji 2005; and references therein), it is plausible that complicated opacity changes will result from shifting dust cloud patterns. The consequent brightness fluctuations will not necessarily be similar in various photometric passbands: this point has been explored by Bailer-Jones (2002).

Nevertheless, similarity of the photometric changes in the *J*, *H* and K_s bands would be a convincing demonstration of real variability.

Table 3. Additional observations to Table 1 that were used in deriving the information in Table 4.

Name	J	H	K_s	Sp.	Date (HJD 245 0000+)	Run length (h)	N(max)	$\sigma(J), \sigma(H), \sigma(K_s)$ (mmag)
EROS-MP J0032−4405	14.78	13.86	13.27	L0:	2592	0.3	3	4, 7, 5
					2891	2.1	10	7, 7, *
DENIS 0255−4700	13.23	12.19	11.53	L8	2888	1.0	4	*, 4, *
2M 2104−1037	13.84	12.98	12.37	L2.5	2801	3.7	40	7, 9, 6
					2888	2.9	13	7, 8, *
2M 2130−0845	14.14	13.33	12.82	L1	2805	3.7	32	5, 6, 10
					2885	4.2	19	5, 19, 14
2M 2158−1550	15.04	13.87	13.19	L4:	2806	4.3	26	5, 4, 6
					2887	0.8	3	9, *, *
ϵ Indi Bab	11.91	11.31	11.21	T1/T6	2803	2.9	31	*, 12, 12
					3281	4.5	67	*, *, 13
					3282	4.4	79	*, 11, 10
2M 2224−0158	14.07	12.82	12.02	L4.5	2804	2.3	17	5, 4, 5
					2891	1.9	19	9, 8, 5

Table 4. Comparison of the photometry from the nights listed in columns 2 and 3. Results for filters J (columns 4–6), H (columns 7–9) and K_s (columns 10–12) are given. For each filter, the first column gives the number of stars used (for the zero-point determination) out of the number available; the second column gives the zero-point offset z and the standard deviation S^* of the scatter around it (both in units of millimagnitudes); and the third column gives an ad hoc significance level (in per cent) for z being non-zero. Significance levels better than 10 per cent are written in bold.

Name	HJD1	HJD2 (245 0000+)	Used	J z (S^*)	α	Used	H z (S^*)	α	Used	K_s z (S^*)	α
EROS-MP J0032−4405	2592	2891	10/12	−12 (14)	46	10/11	4 (16)	75		*	
SSSPM J0109−5101	3277	3278	6/7	−4 (2)	13	9/11	−4 (4)	58	6/7	−16 (9)	13
	3277	3280	7/9	−3 (4)	60	9/11	−4 (4)	42	10/11	−17 (18)	42
	3278	3280	7/7	2 (8)	50	9/11	−3 (2)	17	6/7	−7 (7)	25
DENIS 0255−4700	2888	3282		*		9/9	−23 (41)	50		*	
2M 2104−1037	2801	2888	47/55	8 (11)	64	37/42	7 (28)	86		*	
	2801	3283	55/74	23 (6)	**7**	70/77	11 (9)	33	43/56	4 (7)	67
	2888	3283	21/33	7 (6)	44	28/30	−1 (30)	94		*	
2M 2130−0845	2805	2885	37/40	7 (21)	88	43/50	9 (16)	69	35/39	46 (30)	23
	2805	3277	42/43	13 (10)	27	54/60	12 (13)	48	42/42	5 (19)	84
	2805	3278	36/40	22 (10)	**7**	44/47	19 (9)	**6**	34/37	12 (15)	53
	2885	3277	38/41	7 (17)	69	46/48	−6 (28)	84	34/36	−28 (40)	62
	2885	3278	37/40	18 (24)	56	42/45	6 (19)	76	33/33	−21 (39)	62
	3277	3278	40/45	9 (9)	32	40/54	7 (7)	34	39/43	9 (13)	50
2M 2158−1550	2806	2887	19/23	−11 (12)	54		*			*	
ϵ Ind Bab	2803	3281		*			*		21/22	−57 (30)	**4**
	2803	3282		*		37/43	−34 (8)	**7**	30/31	−53 (24)	**3**
	3281	3282		*			*		25/26	9 (8)	30
2M 2224−0158	2804	2891	6/7	−15 (8)	13	20/21	12 (26)	55	15/17	53 (34)	11

ACKNOWLEDGMENTS

REFERENCES

Ackerman A. S., Marley M. S., 2001, ApJ, 556, 872
Artigau E., Nadeau D., Doyon R., 2003, in Martín E. L., ed., Proc. IAU Symp. 211, Brown Dwarfs. Astron. Soc. Pac., San Francisco, p. 451
Bailer-Jones C. A. L., 2002, A&A, 389, 963
Bailer-Jones C. A. L., Mundt R., 2001, A&A, 367, 218
Burgasser A. J., Marley M. S., Ackerman A. S., Saumon D., Lodders K., Dahn C. C., Harris H. C., Kirkpatrick J. D., 2002, ApJ, 571, L151
Butler C. J., 1991, Mem. Soc. Astron. Italy, 62, 243
Enoch M. L., Brown M. E., Burgasser A. J., 2003, AJ, 126, 1006

Gelino C. R., Marley M. S., Holtzman J. A., Ackerman A. S., Lodders K., 2002, ApJ, 577, 433

Koen C., 2003, MNRAS, 346, 473

Koen C., 2004, MNRAS, 354, 378

Koen C., 2005a, MNRAS, 357, 1151

Koen C., 2005b, MNRAS, in press

Koen C., Matsunaga N., Menzies J., 2004, MNRAS, 354, 466 (Paper I)

Lodieu N., Scholz R.-D., McCaughrean M. J., 2002, A&A, 389, L20

Nagashima C. et al., 1999, in Nakamoto T., ed., Star Formation 1999. Nobeyama Radio Observatory, Nobeyama, p. 397

Schubert G., Zhang K., 2000, in Griffith C. A., Marley M. S., eds, ASP Conf. Ser. Vol. 212, From Giant Planets to Cool Stars. Astron. Soc. Pac., San Francisco, p. 210

Tsuji T., 2005, ApJ, 621, 1033

Woitke P., Helling C., 2004, A&A, 414, 335

This paper has been typeset from a TEX/LATEX file prepared by the author.